Amitriptyline influences the mechanical withdrawal threshold in bone cancer pain rats by regulating glutamate transporter GLAST

Simeng Ma[1], Xiaochun Zheng[1] ⓘ, Ting Zheng[1], Fengyi Huang[1], Jundan Jiang[1], Huirong Luo[1], Qianqian Guo[1], and Bin Hu[1]

Abstract

Patients with cancer, especially breast, prostate, and lung cancer, commonly experience bone metastases that are difficult to manage and are associated with bone cancer pain. Amitriptyline is often used to treat chronic pain, such as neuropathic pain. In this study, the effects of amitriptyline on the mechanical withdrawal threshold and its underlying mechanisms were evaluated in rat models of bone cancer pain. Walker 256 rat mammary gland carcinoma cells were injected into the bone marrow cavity of the right tibia of rats to provoke bone cancer pain. Then, amitriptyline was intraperitoneally administered twice daily from fifth day after the operation. Rats with bone cancer showed an apparent decline in the mechanical withdrawal threshold at day 11 after Walker 256 cells inoculation. The levels of the glutamate-aspartate transporter in the spinal cord dorsal horn decreased remarkably, and the concentration of the excitatory amino acid glutamate in the cerebrospinal fluid increased substantially. Amitriptyline injection could prevent the decline of mechanical withdrawal threshold in bone cancer pain rats. In addition, glutamate-aspartate transporter was upregulated on the glial cell surface, and glutamate levels were reduced in the cerebrospinal fluid. However, amitriptyline injection could not prevent the bone cancer pain-induced reduction in glutamate-aspartate transporter in the glial cell cytosol, it further downregulated cytosolic glutamate-aspartate transporter. Amitriptyline had no significant effect on *GLAST* messenger RNA expression, and bone cancer pain-invoked protein kinase A/protein kinase C upregulation was prevented. Taken together, these results suggest that the intraperitoneal injection of amitriptyline can prevent the decrease of mechanical withdrawal threshold in bone cancer pain rats, the underlying mechanisms may be associated with the inhibition of protein kinase A/protein kinase C expression, thus promoting glutamate-aspartate transporter trafficking onto the glial cell surface and reducing excitatory amino acid concentrations in the cerebrospinal fluid.

Keywords

Amitriptyline, bone cancer pain, GLAST, glutamate, protein kinase A, protein kinase C

Introduction

Bone cancer pain (BCP) is one of the most common clinical symptoms and is difficult to treat effectively,[1] it occurs in patients with primary bone cancer or secondary bone metastasis from distant sites, such as the breast, prostate, and lung.[2] Among patients with terminal breast and prostate cancer, up to 70% exhibit metastasis to the bone tissue[3] and 75% of these patients suffer from severe BCP.[1,4] BCP is a very complicated clinical pain and includes tonic pain or ongoing pain, spontaneous pain, and movement-induced pain,[5–7] severely decreasing quality of life.[8] It may even lead to anxiety, depression, and suicidal tendencies.[6,9] Thus, the treatment of bone cancer is not only limited to improving survival

[1]Fujian Provincial Hospital, Fuzhou, China

Corresponding Author:
Xiaochun Zheng, Fujian Provincial Hospital, Fuzhou 350001, China.
Email: zhengxiaochun7766@163.com

time but also to the relief of cancer pain. Although a variety of treatments, such as nonsteroidal anti-inflammatory drugs, bisphosphonates, radiation, and surgical interventions, are used to alleviate BCP, opioids remain the mainstay analgesic therapy.[10] Opioids eventually result in addiction, tolerance, nausea, and vomiting.[11] Therefore, new therapies for pain relief and further studies of its underlying mechanism are urgently needed in BCP.[12]

Glutamate (Glu) is an important component of excitatory neurotransmitters in the central nervous system and plays critical roles in the transmission of pain signals and the maintenance of sensitization in the pain pathway.[13,14] A reduction in Glu release or receptor-binding ability is accompanied by a loss of hyperalgesia, thus alleviating pain.[14] Extensive research has shown that the maintenance of Glu levels is mainly regulated by glutamate transporters (GTs) on the cell membrane.[15] Glutamate-aspartate transporter (GLAST) is one of the most abundant GTs in the nervous system. It is densely expressed in lamina I and II of the spinal dorsal horn and plays pivotal roles in the transduction of pain signals and formation of hyperalgesia.[16] Several recent studies have suggested that GLAST is a functional receptor involved in the reduction of the pain threshold in rats with BCP, and the upregulation of GLAST expression may be a useful approach to relieve pain induced by bone cancer.

Tricyclic antidepressants (TCAs) are widely used to treat neuropathic pain.[17] Amitriptyline has a clear therapeutic effect on neuropathic pain. This therapeutic effect is mediated by the downregulation of protein kinase A (PKA) and protein kinase C (PKC) in glial cells, resulting in the transport of GLAST from the cytosol to the plasma membrane and eventually enhancing glutamate uptake and decreasing glutamate levels in the cerebrospinal fluid.[18] However, whether amitriptyline relieves BCP through similar or different mechanisms remains to be elucidated. The purpose of this study was to investigate the analgesic effect of the intraperitoneal injection of amitriptyline in BCP rats and the role of PKA/PKC-mediated GLAST regulation.

Materials and methods

Animals

A total of 90 female Sprague–Dawley (SD) rats weighing 200–250 g and 12 female SD rats weighing 60–80 g (provided by the Department of Experimental Animal Center, Fujian Medical University) were used. The adult female SD rats were numbered with tail markings and five animals were housed in each cage, with a 12-h alternating light-dark cycle at $24 \pm 2°C$ with food and water available ad libitum. Rats were randomly divided into the following six groups: (1) a control group (CONT), (2) a sham-operated group (Sham), (3) a bone cancer pain group (BCP), (4) a bone cancer pain, 1.5 mg/kg amitriptyline intraperitoneal injection group ($AMI_{1.5}$), (5) a bone cancer pain, 3 mg/kg amitriptyline intraperitoneal injection group (AMI_3), and (6) a bone cancer pain, 10 mg/kg amitriptyline intraperitoneal injection group (AMI_{10}) (n = 15/group). All experimental procedures and protocols were performed in accordance with the National Institutes of Health guidelines and Ethical Issue of the International Association for the Study of Pain and were reviewed and approved by the Experimental Animal Care and Use Committee of Fujian Provincial Hospital. Efforts were made to minimize suffering and the number of animals used.

Preparation of Walker 256 rat mammary gland carcinoma cells

Female rats weighing 60–80 g were injected with 0.5 mL of 1×10^7 cells/mL Walker 256 cells (Shanghai Jiuzhi Biotechnology Co. Ltd., Shanghai, China) into the abdominal cavity. After seven days, the ascites fluid was collected aseptically. The cells were centrifuged at 1200 r/min for 3 min, washed three times with 10 mL of sterile phosphate-buffered saline (PBS), counted using a hemocytometer, diluted to a concentration of 1×10^6 cells/mL for inoculation, and preserved on ice prior to surgery. For the sham group, the same volume of PBS was prepared for injection.

Rat model of bone cancer pain

The rat model of BCP was established using female SD rats and Walker 256 rat mammary gland carcinoma cells as originally described by Mao-Ying et al.[19] In brief, animals were deeply anesthetized with 10% chloral hydrate (0.6 mL/100 g). The pinch test was used to examine whether the rats were anesthetized completely. The right rear hindlimb of rats was shaved to expose the skin over the tibial plateau, which was sterilized three times with an iodine tincture, and an incision was made, exposing the tibia. Then, 10 μL of Walker 256 carcinoma cells (or 10 μL of PBS without cells in sham animals) was injected into the marrow cavity through a hole drilled on the right tibia. The hole was cautiously closed with bone wax, and then the incision was washed with 75% ethanol to prevent the extraosseous extension of carcinoma cells. Muscle and skin were sutured in separate layers with 4–0 absorbable thread. Animals were intraperitoneally injected with 80,000 U of penicillin to prevent infection. Radiology and hematoxylin and eosin (H&E) staining are used to evaluate the tumor growth. In H&E results, tumor and marrow areas were measured using Image J software.

Measurement of mechanical withdrawal threshold

Mechanical withdrawal threshold (MWT) was tested at day 0 before the operation and on days 4, 7, 11, 14, 17, and 21 after the operation. The rats were placed in a transparent Perspex cage (26 cm × 14 cm × 26 cm) on a 22-cm-high wire mesh platform (each grid of 0.5 cm × 0.5 cm). The MWT was measured according to a previous study,[20] after 30 min of habituation, MWT was assessed using von Frey filaments with a bending force ranging from 0.6 g to 26 g (0.6, 1, 1.4, 2, 4, 6, 8, 10, 15, and 26 g). The number of stimulations for each force was five pokes, and vigorous paw withdrawal, licking, or shaking were taken as positive responses. The minimum force that could provoke at least three withdrawal responses of the right hind paw was defined as the WMT.

CSF sample collection and measurement of EAAs

Cerebrospinal fluid (CSF) was collected with a 1-mL sterile syringe and frozen at −80°C until excitatory amino acid (EAA) measurement by ultraviolet spectrophotometry. All kit components and samples were brought to room temperature (18°C–25°C) before use. Five diluted standards were established—10,000 ng/mL, 3333.3 ng/mL, 1111.1 ng/mL, 370.4 ng/mL, and 123.5 ng/mL—and EP tubes with Standard Diluent as the blank control contained 0 ng/mL. Then, 50 µL each of dilutions of standard, blank, and samples were added to the appropriate wells, and 50 µL of Detection Reagent A was immediately added to each well, followed by gentle shaking. A plate sealer was added and plates were incubated for 1 h at 37°C. The solution was aspirated, 350 µL of 1× Wash Solution was added to each well using a squirt bottle, and the plate was allowed to sit for 1–2 min. The remaining liquid was completely removed from all wells by snapping the plate onto absorbent paper three times. Then, 100 µL of Detection Reagent B working solution was added to each well. Samples were incubated for 30 min at 37°C after they were covered with the Plate Sealer. The aspiration/wash process was repeated a total of five times. A total of 90 µL of Substrate Solution was added to each well. A new Plate Sealer was used to cover samples, followed by incubation for 10–20 min at 37°C in the dark. The liquid turned blue by the addition of Substrate Solution, and 50 µL of Stop Solution was added to each well. The liquid turned yellow by the addition of Stop Solution. Drops of water and fingerprints on the bottom of the plate were removed and a lack of bubbles on the surface of the liquid was confirmed. Then, a microplate reader was used to measure absorbance at 450 nm immediately.

Preparation of spinal cord plasma membrane and cytosolic fractions

Rats were deeply anesthetized with 10% chloral hydrate (0.6 mL/100 g), and the lumbar enlargement was extracted and immediately divided into ventral and dorsal quadrants. Cytoplasmic, Nuclear, and Membrane Compartment Protein Extraction Kits were used to fractionate each dorsal part of the spinal cord into cytosolic, membrane, and nuclear fractions. A total of 400 µL of ice-cold buffer C was added to 200 mg of tissue that was chopped into small pieces. The tissue was homogenized at a moderate speed for 20 s and preserved on ice for a few seconds; homogenization was repeated twice more. The mixture was rotated at 4°C for 20 min. The mixture was centrifuged at 18,000 r/min and 4°C for 20 min. The supernatant was removed and saved in another tube. The supernatant contained cytoplasmic proteins. The pellet was washed with 800 µL of ice-cold buffer W, rotated at 4°C for 5 min, and centrifuged at 18,000 r/min and 4°C for 20 min. The supernatant was drained. Then, 200 µL of ice-cold buffer N was added to the pellet, followed by rotation at 4°C for 20 min and centrifugation at 18,000 r/min and 4°C for 20 min. The supernatant was removed and saved in another tube. The supernatant contained nuclear proteins. Then, 200 µL of ice-cold buffer was added to the pellet, rotated at 4°C for 20 min, and centrifuged at 18,000 r/min and 4°C for 20 min. The supernatant was removed and saved in another tube. The supernatant contained membrane proteins. The proteins were aliquoted and labeled and stored at −80°C.

Western blotting

Cytoplasmic or membrane proteins were unfrozen for GLAST detection, and dorsal parts of the lumbosacral spinal cord were homogenized separately in lysis buffer containing phenylmethylsulfonyl fluoride for PKA/PKC detection. After centrifugation at 1200 g for 20 min at 4°C, supernatants were collected for western blotting. The BCA Protein Assay Kit was used following the manufacturer's instructions for protein detection. After each sample was denatured by heating at 100°C for 10 min in an equal volume of SDS sample buffer, 40 µg of protein was separated on a 10% SDS gel and transferred to a polyvinylidene difluoride membrane. Then, the membrane was blocked with 5% milk and incubated overnight at 4°C with polyclonal guinea pig anti-GLAST (1:2500) antibodies, polyclonal rabbit anti-PKA antibodies (1:1000), or monoclonal mouse anti-PKC (1:2500) antibodies. The membranes were washed with Tris-HCl buffer and incubated with the corresponding secondary antibody, donkey anti-rabbit IgG (1:2500), for 1 h at room temperature.

The chemiluminescence imaging system was used for the visualization of bound antibodies. Data were analyzed using the computer-assisted imaging analysis system.

Real-time quantitative PCR

The lumbar enlargement was removed from anesthetized rats and immediately divided into ventral and dorsal quadrants. Total RNA was extracted from 200 mg of the dorsal part using TRIzol reagent and quantitated using a fluorescence method. The reverse transcription system included 5× M-MLV Buffer (4 μL), RTase M-MLV (RNase H-; 200 U/μL, 0.5 μL), Oligo(dT)18 (0.5 μL), RNase inhibitor (40 U, 0.25 μL), random primer (0.5 μL), and RNase-Free dH$_2$O (14.25 μL). The reverse transcription (RT) protocol was one cycle at 42°C for 60 min and then one cycle at 72°C for 15 min. Quantitative real-time polymerase chain reaction (PCR) was performed using the ViiA7 Real-Time PCR System. The RT-qPCR system included RT product (5 μL), SYBR$^®$ Premix Ex Taq^{TM} (Tli RNaseH Plus; 2×, 10 μL), 10 μM PCR Forward Primer (0.5 μL), 10 μM PCR Reverse Primer (0.5 μL), and dH$_2$O (4 μL). The RT-qPCR protocol was one cycle of polymerase activation for 30 s at 95°C, followed by 40 cycles of denaturation for 5 s at 95°C, annealing for 34 s at 60°C, and extension for 30 s at 72°C. A melting curve analysis was performed. Results were analyzed using PRIMER5/NCBI analysis software. Primer sequences were as follows: *GLAST* 5′-AACCCAAGGGAAG AAAGCCT-3′ (forward), 5orGGCTGTACTCTATTC CGCCT-3CT(reverse); and actin: 5′-TAT CCTGG CCTCACTGTCCA-3′ (forward), 5′-AAGGGTGTA AAACGCAGCTC-3′ (reverse).

Immunocytochemistry and image analysis

Rats were deeply anesthetized with 10% chloral hydrate (0.6 mL/100 g) and then perfused transcardially with 0.1 M phosphate buffer, followed by 4% paraformaldehyde. The lumbar enlargement (L1–L2) was removed and transferred to a 30% sucrose solution in PBS overnight at 4°C. Then, 5-μm sections were cut and air-dried on microscope slides for 30 min at room temperature. The tissue sections were preincubated with 5% normal goat serum and 0.01% Triton X-100 in PBS. The sections were washed in ice-cold PBS three times and incubated with fluorescein isothiocyanate (FITC)-labeled mouse monoclonal anti-GFAP and unlabeled rabbit polyclonal antibodies anti-GLAST in 0.01% Triton X-100, 2% normal goat serum, and PBS overnight at 4°C. Then, the sections were processed with rhodamine-labeled goat anti-rabbit antibody for 1 h at room temperature. Fluorescent images were captured using a fluorescence microscope.

Statistical analyses

SPSS22.0 was used for data analyses. All data were recorded as means ± standard error of the mean. The statistical significance of differences between groups was analyzed using a one-way analysis of variance and the Kruskal–Wallis H test. $P < 0.05$ was considered statistically significant.

Results

Induction of the Walker 256-induced bone cancer pain model

MWT values on postoperative days 0, 4, 7, 11, 14, 17, and 21 were used to assess the pain induced by bone cancer (Figure 1). The baseline MWT value did not differ significantly among groups ($P > 0.05$). No significant difference in MWT was observed between rats that received operations and those in the CONT group ($P > 0.05$), suggesting that the operation alone did not significantly alter the MWT. In the BCP group, the MWT was significantly lower on seven days after the operation than that of the CONT group ($P < 0.05$). Tumor cells at the injection site were observed by H&E staining on 21 days after the operation (Figure 2). In the CONT group, a normal bone structure was observed, and the clear border of trabecular bone was filled with bone marrow cells. In contrast, the tibia of BCP rats was destroyed and the medullary cavity was filled with carcinoma cells, instead of bone marrow cells. The result of cancer cell marrow occupancy measured by Image J software is 25.3%. To investigate the bone destruction, the bone mineral density was examined by X-ray on days 0, 7, 14, and 21 after Walker 256 cell
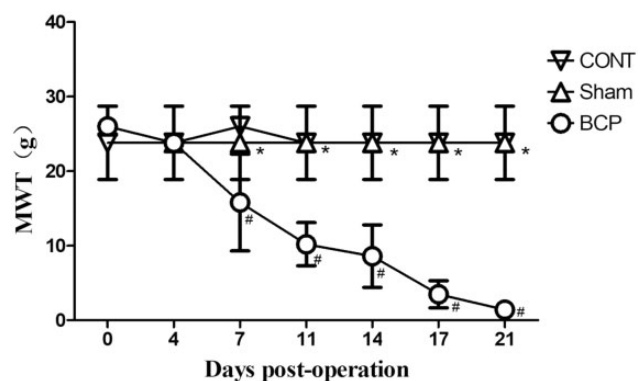
Figure 1. Transplantation of Walker 256 mammary carcinoma cells induced a decrease in the MWT after surgery. MWT did not show a significant difference between the CONT and Sham groups (*$P > 0.05$). MWT was significantly lower in the BCP group than in the CONT group (#$P < 0.05$). The difference was significant on day 7 and was maintained until day 21. MWT: mechanical withdrawal threshold; BCP: bone cancer pain; CONT: control group.

injection into the marrow cavity of the tibia (Figure 3). There was no detectable bone loss on day 0; however, a significant decrease of bone mineral density was observed on day 7, destruction of the bone cortex was observed on day 14, and the pathological fracture eventually appeared on day 21. Therefore, the MWT, radiographic, and pathological results all clearly confirmed that carcinoma cells induced bone destruction and BCP.
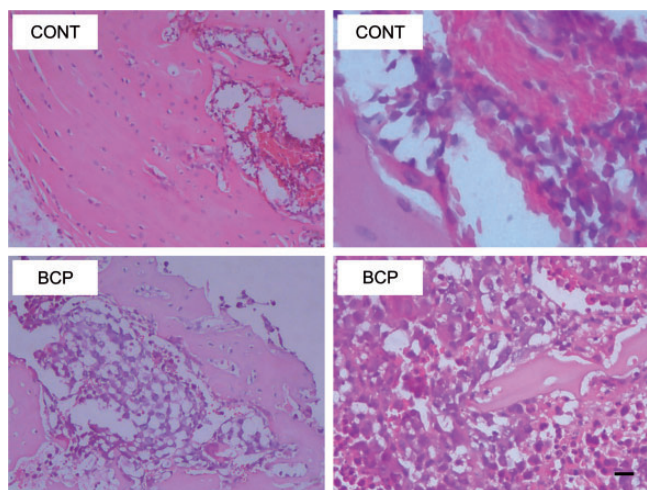
Figure 2. Increase in carcinoma cells in the tibia of BCP rats. The CONT rats showed a normal bone structure, and a clear border of the trabecular bone was filled with bone marrow cells. In contrast, the tibia of BCP rats was destroyed, and the medullary cavity was filled with carcinoma cells instead of bone marrow cells, the cancer cell marrow occupancy is 25.3%. Scale bar represents 10 μm. BCP: bone cancer pain; CONT: control group.

Changes in the MWT after amitriptyline injection

The MWT values for the BCP, $AMI_{1.5}$, AMI_3, and AMI_{10} groups on days 0, 4, 7, 11, 14, 17, and 21 were measured. No significant difference in MWT was observed in the $AMI_{1.5}$ animals compared to that in the BCP group animals. However, higher MWT values were observed in the AMI_3 and AMI_{10} groups on days 7, 11, 14, 17, 21 than in the BCP group ($P < 0.05$), and the MWT in the AMI_{10} group was even higher on days 17 and 21 than those in the AMI_3 group ($P < 0.05$) (Figure 4).

Amitriptyline treatment suppresses the BCP-evoked glutamate release

The glutamate concentration in the CSF in the CONT group did not differ significantly from that in the Sham group on days 7, 14, and 21 ($P > 0.05$). The glutamate concentration was significantly higher in the BCP group than in CONT or Sham rats ($P < 0.05$). Intraperitoneal injection with amitriptyline twice daily at 1.5, 3, and 10 mg/kg resulted in increased glutamate concentrations compared with those in BCP rats in a dose-dependent manner ($P < 0.05$) (Figure 5).

Amitriptyline treatment modulates the GLAST concentration in BCP rats

Western blotting was used to evaluate GLAST on the glia cell membrane or cytosol of the spinal cord dorsal horn in the six treatment groups (Figure 6). Neither
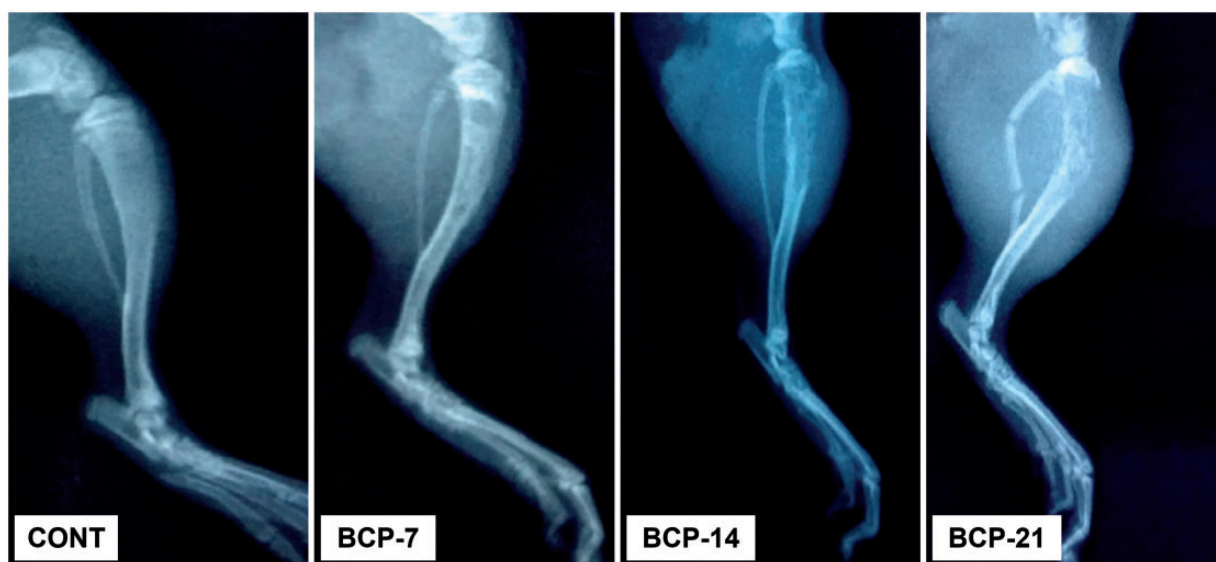
Figure 3. Radiological confirmation of tumor development in the tibia of rats injected with Walker 256 cells. Reduced bone mineral density in bone X-rays indicated that the carcinoma cells induced bone destruction. Rats had no detectable bone loss on day 0, the ipsilateral tibia displayed bone loss on day 7, destruction of bone cortex was observed on day 14, and the pathological fracture appeared on day 21.
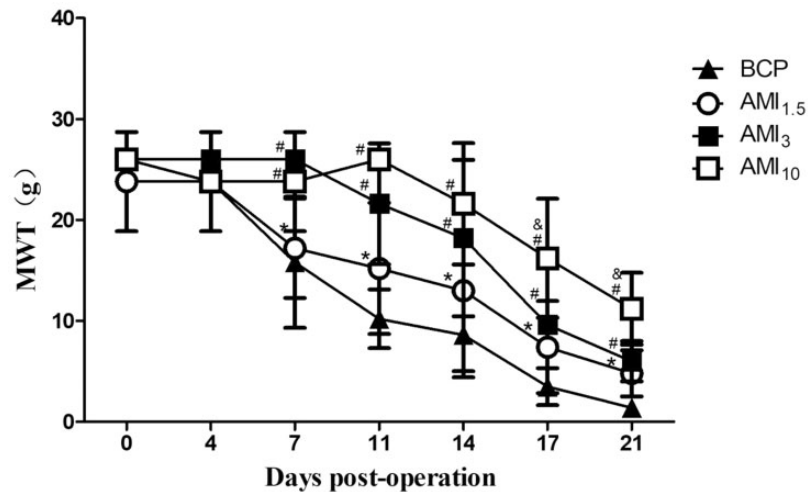
Figure 4. Effects of AMI treatment on the MWT in BCP rats. Rats received AMI or normal saline twice daily from day 5 to day 21 after the inoculation of carcinoma cells. MWT was measured on postoperative days 0, 4, 7, 11, 14, 17, and 2l. No significant change in MWT was observed in the AMI 15 animals compared to that in the BCP group animals (*$P > 0.05$). However, an increased MWT was observed in the AMI3 and AMI 10 groups on days 7, 11, 14, 17, and 21 compared to that in the BCP group (#$P < 0.05$), and MWT values in the AMI 10 group were even higher on days 17 and 21 than those in the AMI3 group (&$P < 0.05$).
MWT: mechanical withdrawal threshold; BCP: bone cancer pain; AMI: amitriptyline.
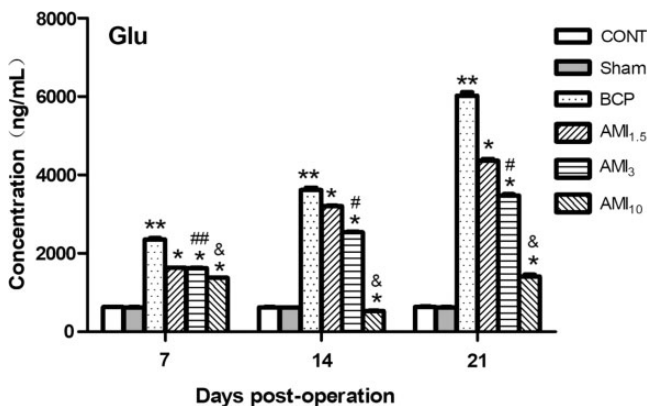
Figure 5. Amitriptyline treatment suppresses BCP-evoked glutamate release. The glutamate concentration in the CSF was detected on postoperative days 7, 14, and 2l. There were no significant differences between the CONT group and Sham group. There was a significant increase in the glutamate concentration in the BCP group compared to CONT or Sham rats (**$P < 0.05$). Intraperitoneal injection with amitriptyline twice daily at 1.5, 3, and 10 mg/kg increased the glutamate concentration compared with that in the BCP rats in a dose-dependent manner (*$P < 0.05$).
BCP: bone cancer pain; CONT: control group; Glu: glutamate; AMI: amitriptyline.

membrane nor cytosolic GLAST levels in the CONT group were significantly different from those in the Sham group ($P > 0.05$). In the BCP group, GLAST on the membrane or cytosol was significantly downregulated compared with that in the CONT or Sham group on days 7 and 21 ($P < 0.05$). Treatment with

amitriptyline at 1.5, 3, and 10 mg/kg upregulated GLAST on the membrane in a dose-dependent manner compared with levels in the BCP group ($P < 0.05$). However, the cytosolic levels of GLAST were remarkably decreased compared with those in the BCP group ($P < 0.05$), and there was no difference between the $AMI_{1.5}$ and AMI_3 group ($P > 0.05$) (Figure 6). Fluorescence microscopy showed that in the CONT group, GLAST was extensively distributed on entire astrocytes but was downregulated in BCP rats. Treatment with amitriptyline resulted in the trafficking of GLAST to the cell surface (Figure 7).

Amitriptyline treatment downregulates PKA/PKC in BCP rats

The PKA and PKC expression levels in the spinal cord dorsal horn on day 21 were measured by western blotting (Figure 8). No significant change in PKA/PKC expression was observed in the Sham group on day 21 compared to that in the CONT group ($P > 0.05$). PKA/ PKC was significantly higher in BCP rats than in CONT or Sham rats ($P < 0.05$). All three doses of amitriptyline (1.5, 3, and 10 mg/kg) produced significant decreases in PKA/PKC in the dorsal spinal cord ($P < 0.05$). Although the AMI_3 group showed a greater decrease in PKA/PKC expression than that in the $AMI_{1.5}$ group, the difference between groups was not statistically significant on day 21 after the operation ($P > 0.05$). The AMI_{10} group showed a significant downregulation
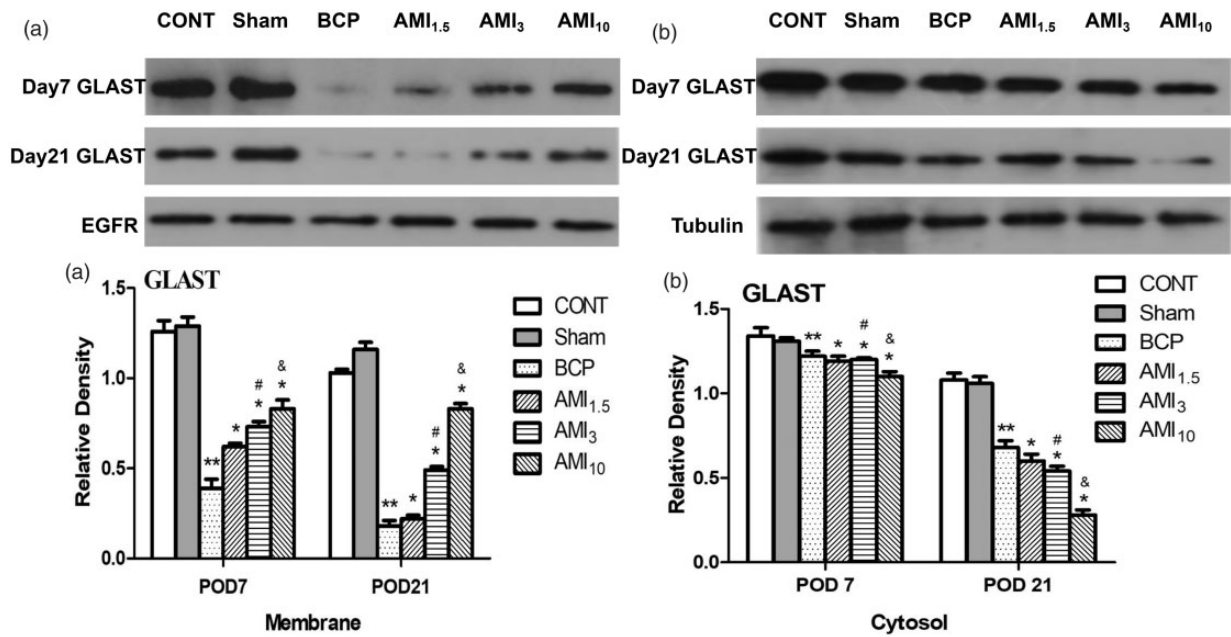
Figure 6. Amitriptyline treatment promotes the trafficking of GLAST from the cytosol to the cell surface in BCP rats. A western blot analysis of GLAST was performed in cytosolic and plasma membrane fractions from the rat spinal cord dorsal horn. Upper panels: anti-EGFR and anti-tubulin antibodies were used as equal loading markers of cytosol and membrane fractions, respectively. Neither membrane nor cytosol GLAST levels in the CONT group differed significantly from those in the Sham group. In the BCP group, GLAST on the membrane or cytosol was significantly downregulated compared with levels in the CONT or Sham group on days 7 and 21 (**$P < 0.05$). Treatment with amitriptyline at 1.5, 3, and 10 mg/kg upregulated GLAST on the membrane in a dose-dependent manner compared to that in the BCP group (*$P < 0.05$, #$P < 0.05$, &$P < 0.05$) (Al and A2). However, the cytosolic levels of GLAST were remarkably lower than those in the BCP group (*$P < 0.05$), and AMI1.5 or AMI3 groups had no significant difference (#$P > 0.05$, &$P > 0.05$) (B1 and B2). BCP: bone cancer pain; CONT: control group; GLAST: glutamate-aspartate transporter; AMI: amitriptyline.

in PKA/PKC expression compared with levels in the AMI$_{1.5}$ and AMI$_3$ groups ($P < 0.05$).

Amitriptyline does not affect the BCP-induced GLAST *mRNA decrease in BCP rats*

We evaluated whether amitriptyline influences *GLAST* messenger RNA (mRNA) expression in BCP rats after 7, 14, and 21 days (Figure 9). Reverse transcription polymerase chain reaction (RT-PCR) analyses indicated that *GLAST* mRNA levels did not differ between the CONT and Sham groups ($P > 0.05$). The level of *GLAST* mRNA in the BCP group decreased remarkably compared with that in the CONT group in a time-dependent manner ($P < 0.05$). No significant difference in *GLAST* mRNA expression was observed in the AMI$_{1.5}$, AMI$_3$, and AMI$_{10}$ group animals on days 7, 14, and 21 compared to that in the BCP group animals ($P < 0.05$).

Discussion

Considerable effort has focused on the development of novel approaches to alleviating BCP. However, therapeutic strategies for alleviating cancer pain are still

often inadequate.[21,22] In this study, the analgesic effect of the intraperitoneal injection twice daily of amitriptyline (1.5, 3, and 10 mg/kg)[23] was evaluated in a BCP rat model developed by injecting Walker 256 carcinoma cells into the tibias of female SD rats. The results suggested that amitriptyline is effective for the management of BCP. Amitriptyline suppresses the BCP-evoked increased expression of PKA/PKC in the spinal cord dorsal horn, promoted the transport of GLAST from the cytosol onto the cell surface, and thus decreased glutamate concentration in the CSF to alleviate BCP.

Animal models of BCP have been established for many years. The results of this study showed that Walker 256 carcinoma cells inoculated into the right hind tibia of female SD rats produce mechanical hyperalgesia, as measured by Von Frey filaments, as well as bone destruction, as detected by X-ray radiography and pathematology. The MWT values decreased and the ipsilateral tibia displayed bone loss on day 7 after surgery; normal bone marrow cells in the medullary cavity were replaced with carcinoma cells, indicating that the model of BCP was successfully established.

Glutamate is the major excitatory neurotransmitter in the central nervous system, including the spinal cord,
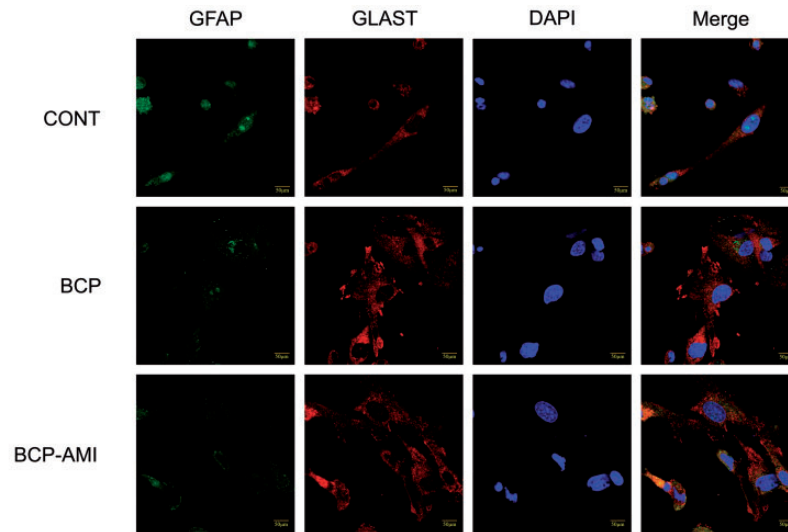
Figure 7. Amitriptyline regulates GLAST trafficking. Spinal cords were labeled with the FITC-labeled mouse monoclonal anti-GFAP antibody (green for astrocytes), unlabeled rabbit polyclonal anti-GLAST antibody (red), or DAPI (blue for nuclei), and fluorescent images were captured using a fluorescence microscope. The laser wavelength was set to 488 nm for FITC fluorescence and 568 nm for rhodamine fluorescence. In the CONT group, GLAST was extensively distributed on the entire astrocyte, but GLAST was downregulated in BCP rats. Treatment with amitriptyline resulted in the trafficking of GLAST to the cell surface. Scale bar represents 50 μm. BCP: bone cancer pain; CONT: control group; GLAST: glutamate-aspartate transporter; GFAP: glial fibrillary acidic protein; DAPI: 4′,6-diamidino-2-phenylindole; AMI: amitriptyline.
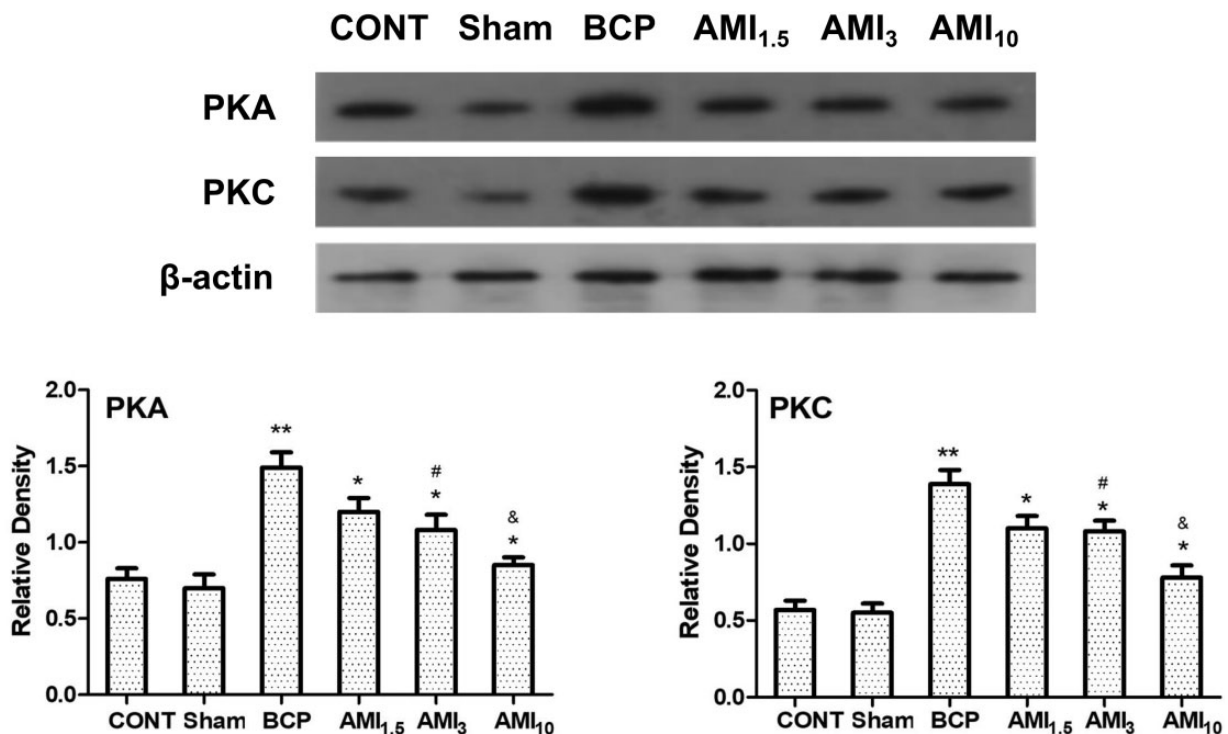
Figure 8. Amitriptyline treatment prevents the upregulation of PKA and PKC expression in BCP rat spinal cords. No significant change in PKA/PKC expression was observed in the Sham group animals on day 21 compared to that in the CONT group animals. PKA/PKC levels were significantly higher in BCP rats than in CONT or Sham rats ($**P < 0.05$). All three doses of the amitriptyline (1.5, 3, and 10 mg/kg) produced a significant decrease in *PKA/PKC* in the dorsal spinal cord ($*P < 0.05$). The AMI10 group showed significantly lower levels of PKA/PKC expression than those in the AMI1.5 and AMI3 groups ($\&P < 0.05$).
BCP: bone cancer pain; CONT: control group; PKC: protein kinase C; PKA: protein kinase A; AMI: amitriptyline.
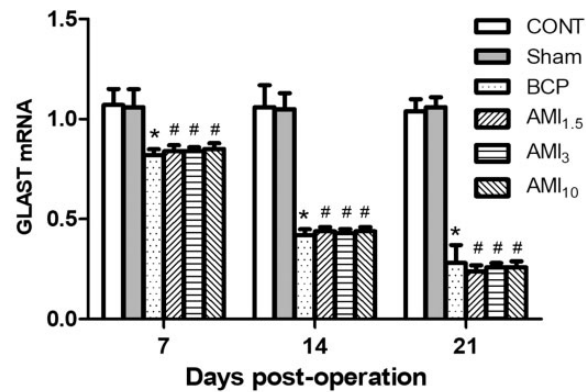
Figure 9. Amitriptyline treatment had no influence on the BCP-induced decrease in GLAST mRNA in BCP rats. The GLAST mRNA levels did not differ between the CONT and Sham groups. The level of GLAST mRNA in the BCP group decreased compared with that in the CONT group in a time-dependent manner (*$P < 0.05$). No significant change in GLAST mRNA expression was observed in the AMI1.5, AMI3, and AMI10 groups compared to that in the BCP group (#$P > 0.05$). BCP: bone cancer pain; CONT: control group; GLAST: glutamate-aspartate transporter; AMI: amitriptyline.

and is involved in pain modulation.[24,25] It plays a key role in the central propagation of pain.[26] Rothstein et al. proved that the GTs GLAST, GLT-1, and EAAC1 account for the majority of functional glutamate transport and are crucial for maintaining homeostasis of extracellular glutamate to prevent chronic glutamate neurotoxicity.[27] EAATs, including GLAST and GLT-1 located on glial cell membranes, take up the majority of glutamate in the synaptic cleft and decrease the release of glutamate to other synapses.[28] Previous studies have demonstrated that the increased expression of GLAST on the plasma membrane, and not the total amount of GLAST, may be involved in the improvement of glutamate uptake activity.[29] GLT-1 trafficking in astrocyte processes could also provide an important and dynamic mechanism for maintaining the local glutamate concentration at the synapse.[30] Peripheral nociceptive signals are processed in the dorsal root ganglion and switched over to the central nervous system in lamina I and II of the spinal cord. Niederberger et al. demonstrated that the GT GLAST is expressed in lamina I and II of the spinal cord, suggesting that GLAST is related to nociceptive transmission.[16] In our study, the downregulation of GLAST on the membrane of the spinal cord dorsal horn and an increase in glutamate in the CSF were observed in BCP rats, resulting in an increase of MWT, suggesting that GLAST is also involved in the development of BCP.

TCAs are commonly used to treat major depressive disorders as well as chronic pain states, such as neuropathic and inflammatory pains.[17,31] Amitriptyline is the most widely used TCA, and its analgesic efficacy has been established for a variety of chronic pain syndromes.[32] Abdel-Salam et al. compared the antinociceptive effects of different classes of antidepressant drugs, including amitriptyline, imipramine, clomipramine, trazodone, and fluoxetine, by carrageenan paw edema and tail-electric stimulation assays in rats, and proved that all antidepressant drugs have antinociceptive properties. Amitriptyline is the strongest analgesic among these drugs and has been a first-line treatment for neuropathic pain for many years.[31,33] Therefore, amitriptyline was chosen in our study. Paudel et al. found that amitriptyline also has analgesic activity in the acute pain state in mice, and its combination with morphine has better antinociceptive effects in the Hot-Plate test than those of morphine alone.[34] Lin et al. found that amitriptyline suppresses the increase in EAA concentrations in spinal CSF dialysates and reverses GT expression, thus preserving the antinociceptive effect of morphine in pertussis toxin-treated rats.[35] Similarly, Tai et al. proved that acute amitriptyline treatment preserves the antinociceptive effect of morphine in morphine-tolerant rats developed by the intrathecal injection of morphine (15 μg/h) for five days, and its underlying mechanisms may involve the downregulation of phospho-PKA and PKC expression, thus inducing GLAST and GLT-1 trafficking onto the glial cell surface, which promotes EAA uptake from the synaptic cleft and reduces the EAA concentration in the spinal CSF.[18] In this study, we found that the intraperitoneal injection of amitriptyline prevented the reduction of MWT in BCP rats, upregulated membrane-type GLAST in the spinal cord dorsal horn, and decreased the concentration of glutamate in the CSF. Tai et al. proved that total level of the astrocyte-type GLAST in the spinal cord dorsal horn are unaffected by amitriptyline injection in rats, but they did not prove it on mRNA level.[18] In our study, no significant difference in *GLAST* mRNA expression was observed in the AMI$_{1.5}$, AMI$_3$, and

AMI$_{10}$ group animals on days 7, 14, and 21 compared to that in the BCP group animals, demonstrate that the amitriptyline injection did not prevent the downregulation of *GLAST* mRNA in BCP rats. We also found that amitriptyline even decreased the cytosolic levels of GLAST. The results suggest that intraperitoneal injection of amitriptyline did not prevent the downregulation of GLAST expression in BCP rats but promoted the trafficking of GLAST from the cytosol to the cell surface, thus increasing glutamate uptake from the synaptic cleft and decreasing the glutamate concentration in the CSF.

Many studies have demonstrated that the effect of amitriptyline on GTs might be associated with PKA and PKC expression. Tai et al. proved that the intrathecal injection of amitriptyline prevents the expression of PKCα, βII, γ, and phospho-PKA in the spinal cord of morphine-tolerant rats.[18] Kalandadze et al. proved that PKC activation results in a rapid redistribution of GLT-1 from the cell surface.[36,37] Zhang et al. and Guillet et al. demonstrated that human cytomegalovirus infection could modulate glutamate uptake and the expression levels of GLAST and GLT-1 via PKC signaling, suggesting that the trafficking of GTs can be regulated by PKA and PKC-dependent signaling pathways and could therefore control total glutamate uptake activity.[38,39] Conversely, increasing the activity and post-translational modifications of GLAST has also been observed by PKC activation.[40] We used a BCP rat model and found the reduction of PKA and PKC expression in the spinal cord dorsal horn after intraperitoneal injection of amitriptyline. This effect involves the regulation of GLAST trafficking from the cytosol to the plasma membrane, consistent with the results of previous studies. But it cannot be directly proved that amitriptyline causes the decrease of PKA and PKC because we did not have intervention for PKA nor PKC with inhibitor and it remains to be further study.

In conclusion, our results suggest that the downregulation of GLAST on the membrane in BCP rats results in a significant reduction of glutamate in the CSF, and this change can be prevented by the intraperitoneal injection of amitriptyline. With respect to the underlying mechanism, it is possible that amitriptyline prevents the upregulation of PKA and PKC, thereby promoting the trafficking of GLAST from the cytosol to the plasma membrane of glial cells in the spinal cord dorsal horn, increasing glutamate uptake from the synaptic cleft, and reducing the glutamate concentration in the CSF. These results suggest that the upregulation of glutamate via the downregulation of GLAST on the membrane is a potential mechanism and therapeutic target for BCP, and amitriptyline may be an effective treatment for BCP.

ORCID iD

Xiaochun Zheng https://orcid.org/0000-0002-6213-0789

References

1. Fidler MM, Soerjomataram I, Bray F. A global view on cancer incidence and national levels of the human development index. *Int J Cancer* 2016; 139: 2436–2446.
2. Goblirsch MJ, Zwolak P, Clohisy DR. Advances in understanding bone cancer pain. *J Cell Biochem* 2005; 96: 682–688.
3. Xu Y, Liu J, He M, Liu R, Belegu V, Dai P, Liu W, Wang W, Xia Q-J, Shang F-F, Luo C-Z, Zhou X, Liu S, McDonald JW, Liu J, Zuo Y-X, Liu F, Wang T-H. Mechanisms of PDGF siRNA-mediated inhibition of bone cancer pain in the spinal cord. *Sci Rep* 2016; 6: 27512.
4. Shenoy P A, Kuo A, Vetter I, Smith M T. The Walker 256 breast cancer cell-induced bone pain model in rats. *Front Pharmacol* 2016; 7: 286.
5. Yanagisawa Y, Furue H, Kawamata T, Uta D, Yamamoto J, Furuse S, Katafuchi T, Imoto K, Iwamoto Y, Yoshimura M. Bone cancer induces a unique central sensitization through synaptic changes in a wide area of the spinal cord. *Mol Pain* 2010; 6: 38.
6. Portenoy RK, Payne D, Jacobsen P. Breakthrough pain: characteristics and impact in patients with cancer pain. *Pain* 1999; 81: 129–134.
7. Mantyh PW. A mechanism based understanding of cancer pain. *Pain* 2002; 96: 1–2.
8. Mantyh PW. Cancer pain and its impact on diagnosis, survival and quality of life. *Nat Rev Neurosci* 2006; 7: 797–809.
9. Hao W, Chen L, Wu L-F, Yang F, Niu J-X, Kaye A D, Xu S-Y. Tanshinone IIA exerts an antinociceptive effect in rats with cancer-induced bone pain. *Pain Physician* 2016; 19: 465–476.
10. Guo G, Peng Y, Xiong B, Liu D, Bu H, Tian X, Yang H, Wu Z, Cao F, Gao F. Involvement of chemokine CXCL11 in

the development of morphine tolerance in rats with cancer-induced bone pain. *J Neurochem* 2017; 141: 553–564.

11. Wang JJ. A survey of cancer pain status in Shanghai. *Oncology* 2008; 74 Suppl 1: 13–18.

12. Hu S, Mao-Ying QL, Wang J, Wang ZF, Mi WL, Wang XW, Jiang JW, Huang YL, Wu GC, Wang YQ. Lipoxins and aspirin-triggered lipoxin alleviate bone cancer pain in association with suppressing expression of spinal proin-flammatory cytokines. *J Neuroinflammation* 2012; 9: 278.

13. Wang H, Kohno T, Amaya F, Brenner GJ, Ito N, Allchorne A, Ji R-R, Woolf CJ. Bradykinin produces pain hypersensitivity by potentiating spinal cord glutamatergic synaptic transmission. *J Neurosci* 2005; 25: 7986–7992.

14. Hartmann B, Ahmadi S, Heppenstall PA, Lewin GR, Schott C, Borchardt T, Seeburg PH, Zeilhofer HU, Sprengel R, Kuner R. The AMPA receptor subunits GluR-A and GluR-B reciprocally modulate spinal synaptic plasticity and inflammatory pain. *Neuron* 2004; 44: 637–650.

15. Gegelashvili G, Robinson MB, Trotti D, Rauen T. Regulation of glutamate transporters in health and disease. *Prog Brain Res* 2001; 132: 267–286.

16. Niederberger E, Schmidtko A, Coste O, Marian C, Ehnert C, Geisslinger G. The glutamate transporter GLAST is involved in spinal nociceptive processing. *Biochem Biophys Res Commun* 2006; 346: 393–399.

17. Sawynok J, Reid AR, Esser MJ. Peripheral antinociceptive action of amitriptyline in the rat formalin test: involvement of adenosine. *Pain* 1999; 80: 45–55.

18. Tai Y-H, Wang Y-H, Tsai R-Y, Wang J-J, Tao P-L, Liu T-M, Wang Y C, Wong C-S. Amitriptyline preserves mor-phine's antinociceptive effect by regulating the glutamate transporter GLAST and GLT-1 trafficking and excitatory amino acids concentration in morphine-tolerant rats. *Pain* 2007; 129: 343–354.

19. Mao-Ying Q-L, Zhao J, Dong Z-Q, Wang J, Yu J, Yan M-F, Zhang Y-Q, Wu G-C, Wang Y-Q. A rat model of bone cancer pain induced by intra-tibia inoculation of Walker 256 mammary gland carcinoma cells. *Biochem Biophys Res Commun* 2006; 345: 1292–1298.

20. Liu X, Bu H, Liu C, Gao F, Yang H, Tian X, Xu A, Chen Z, Cao F, Tian Y. Inhibition of glial activation in rostral ventromedial medulla attenuates mechanical allodynia in a rat model of cancer-induced bone pain. *J Huazhong Univ Sci Technol [Med Sci]* 2012; 32: 291–298.

21. Luo J, Huang X, Li Y, Li Y, Xu X, Gao Y, Shi R, Yao W, Liu J, Ke C. GPR30 disrupts the balance of GABAergic and glutamatergic transmission in the spinal cord driving to the development of bone cancer pain. *Oncotarget* 2016; 7: 73462–73472.

22. Honore P, Mantyh PW. Bone cancer pain: from mecha-nism to model to therapy. *Pain Med* 2000; 1: 303–309.

23. LaBuda CJ, Little PJ. Pharmacological evaluation of the selective spinal nerve ligation model of neuropathic pain in the rat. *J Neurosci Methods* 2005; 144: 175–181.

24. Ren BX, Gu XP, Zheng YG, Liu CL, Wang D, Sun YE, Ma ZL. Intrathecal injection of metabotropic glutamate receptor subtype 3 and 5 agonist/antagonist attenuates bone cancer pain by inhibition of spinal astrocyte

activation in a mouse model. *Anesthesiology* 2012; 116: 122–132.

25. Fundytus ME. Glutamate receptors and nociception: implications for the drug treatment of pain. *CNS Drugs* 2001; 15: 29–58.

26. Fazzari J, Lin H, Murphy C, Ungard R, Singh G. Inhibitors of glutamate release from breast cancer cells; new targets for cancer-induced bone-pain. *Sci Rep* 2015; 5: 8380.

27. Rothstein JD, Dykes-Hoberg M, Pardo CA, Bristol LA, Jin L, Kuncl RW, Kanai Y, Hediger MA, Wang Y, Schielke JP, Welty DF. Knockout of glutamate transporters reveals a major role for astroglial transport in excitotoxicity and clearance of glutamate. *Neuron* 1996; 16: 675–686.

28. Diamond JS, Jahr CE. Synaptically released glutamate does not overwhelm transporters on hippocampal astro-cytes during high-frequency stimulation. *J Neurophysiol* 2000; 83: 2835–2843.

29. Ikegaya Y, Matsuura S, Ueno S, Baba A, Yamada M K, Nishiyama N, Matsuki N. Beta-amyloid enhances glial glutamate uptake activity and attenuates synaptic efficacy. *J Biol Chem* 2002; 277: 32180–32186.

30. Zhou J, Sutherland ML. Glutamate transporter cluster formation in astrocytic processes regulates glutamate uptake activity. *J Neurosci* 2004; 24: 6301–6306.

31. Abdel-Salam OME, Nofal SM, El-Shenawy SM. Evaluation of the anti-inflammatory and anti-nociceptive effects of different antidepressants in the rat. *Pharmacological Res* 2003; 48: 157–165.

32. Robinson LR, Czerniecki JM, Ehde DM, Edwards WT, Judish DA, Goldberg ML, Campbell KM, Smith DG, Jensen MP. Trial of amitriptyline for relief of pain in amputees: results of a randomized controlled study. *Arch Phys Med Rehabil* 2004; 85: 1–6.

33. Moore RA, Derry S, Aldington D, Cole P, Wiffen PJ. Amitriptyline for neuropathic pain in adults. *Cochrane Database Syst Rev* 2015; 7: CD008242.

34. Paudel KR, Das BP, Rauniar GP, Sangraula H, Deo S, Bhattacharya SK. Antinociceptive effect of amitriptyline in mice of acute pain models. *Indian J Exp Biol.* 2007;45:529–531.

35. Lin J-A, Tsai R-Y, Lin Y-T, Lee M-S, Cherng C-H, Wong C-S, Tzeng J-I. Amitriptyline pretreatment preserves the antinociceptive effect of morphine in pertussis toxin-treated rats by lowering CSF excitatory amino acid con-centrations and reversing the downregulation of glutamate transporters. *Brain Res* 2008; 1232: 61–69.

36. Kalandadze A, Wu Y, Robinson MB. Protein kinase C activation decreases cell surface expression of the GLT-1 subtype of glutamate transporter. Requirement of a carboxyl-terminal domain and partial dependence on serine 486. *J Biol Chem* 2002; 277: 45741–45750.

37. García-Tardón N, González-González IM, Martínez-Villarreal J, Fernández-Sánchez E, Giménez C, Zafra F. Protein kinase C (PKC)-promoted endocytosis of gluta-mate transporter GLT-1 requires ubiquitin ligase Nedd4-2-dependent ubiquitination but not phosphoryla-tion. *J Biol Chem* 2012; 287: 19177–19187.

38. Zhang L, Li L, Wang B, Qian D-M, Song X-X, Hu M. HCMV induces dysregulation of glutamate uptake and transporter expression in human fetal astrocytes. *Neurochem Res* 2014; 39: 2407–2418.

39. Guillet B, Velly L, Canolle B, Masmejean F, Nieoullon A, Pisano P. Differential regulation by protein kinases of activity and cell surface expression of glutamate transporters in neuron-enriched cultures. *Neurochem Int* 2005; 46: 337–346.

40. Susarla BTS, Seal RP, Zelenaia O, Watson DJ, Wolfe JH, Amara SG, Robinson MB. Differential regulation of GLAST immunoreactivity and activity by protein kinase C: evidence for modification of amino and carboxyl termini. *J Neurochem* 2004; 91: 1151–1163.